P-Ge/Sn π-Interactions Versus Arene…Ge/Sn Contacts for the Stabilization of Diphosphatetrylenes, $(R_2P)_2E$ (E = Ge, Sn)

Keith Izod,* Peter Evans, Paul G. Waddell

Main Group Chemistry Laboratories, School of Chemistry, Newcastle University, Newcastle upon Tyne, NE1 7RU, UK; e-mail: keith.izod@ncl.ac.uk

Abstract

The diphosphatetrylenes {(Dipp)(R')P}$_2$E [R' = Mes, E = Ge (**1Ge**), Sn (**1Sn**); R' = CH(SiMe$_3$)$_2$, E = Sn (**2Sn**)] have been isolated and characterized by multinuclear and variable temperature NMR spectroscopy and X-ray crystallography [Dipp = 2,6-*i*Pr$_2$C$_6$H$_3$, Mes = 2,4,6-Me$_3$C$_6$H$_2$]. All three compounds crystallize as discrete monomers with two pyramidal phosphorus centers. However, variable-temperature ^{31}P{^{1}H} NMR spectroscopy indicates that both **1Ge** and **2Sn** are subject to dynamic exchange between this form and a form containing one planar and one pyramidal phosphorus center in solution. In contrast, **1Sn** retains two pyramidal phosphorus centers in solution and exhibits no evidence for exchange with a form containing a planar phosphorus center. The related compound [{(Me$_3$Si)$_2$CH}$_2$P]$_2$Sn (**3Sn**) was isolated in very low yield and was shown by X-ray crystallography to possess one planar and one pyramidal phosphorus center in the solid state. DFT calculations reveal that the conformations of **1Ge**, **1Sn**, and **2Sn** observed in the solid state are significantly stabilized by the delocalization of electron density from the aromatic rings into the vacant p-orbital at the tetrel center. Thus, for diphosphatetrylenes possessing aromatic substituents at phosphorus, stabilization may be achieved by two competing mechanisms: (i) planarization of one phosphorus center and consequent delocalization of the phosphorus lone pair into the vacant tetrel p-orbital, or (ii) pyramidalization of both phosphorus centers and delocalization of aromatic π-electron density into the tetrel p-orbital. For **3Sn**, which lacks aromatic groups, only the former stabilization mechanism is possible.

Introduction

While diaminocarbenes and their heavier group 14 analogues (diaminotetrylenes (R$_2$N)$_2$E; E = Si, Ge, Sn, Pb) are well known,[1] the chemistry of the corresponding phosphorus-substituted species (diphosphacarbenes (R$_2$P)$_2$C and diphosphatetrylenes (R$_2$P)$_2$E) is much less well

developed.[2-9] This may chiefly be attributed to the large barrier to planarization of phosphorus compared to nitrogen (for comparison, the inversion barriers of NH_3 and PH_3 are approximately 25 and 150 kJ mol^{-1}, respectively),[10] which inhibits π-overlap between the phosphorus lone pair(s) and the vacant p-orbital at the tetrel center, barring one of the primary means of stabilization of these species. Nonetheless, a small number of diphosphacarbenes and an increasing number of diphosphatetrylenes have been reported.[2-9] While the known diphosphacarbenes exhibit near-planar phosphorus centers (and consequent P=C π-overlap),[2] the corresponding diphosphatetrylenes are typically isolated as dimers containing a P_2E_2 core (**A**), or else as monomers containing pyramidal phosphorus centers (**B**),[3-9] which do not exhibit any tendency towards P=E π-interactions; until recently, diphosphatetrylenes containing a planar phosphorus center (**C**) were unknown (Chart 1).

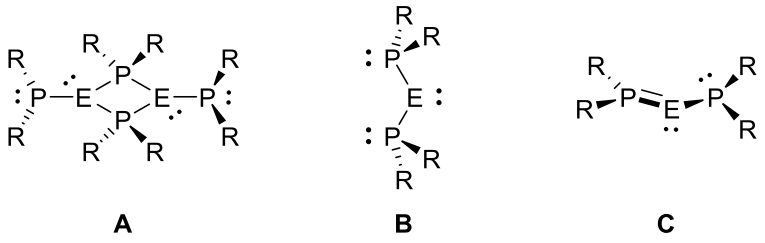

Chart 1

In this regard, we recently reported the first example of a diphosphagermylene [{(Dipp)$_2$P}$_2$Ge] (**I**) that is stabilized by a Ge=P π-interaction and have subsequently shown that a similarly-stabilized diphosphastannylene [{(Dipp)$_2$P}$_2$Sn] (**II**) is accessible [Dipp = 2,6-*i*Pr$_2$C$_6$H$_3$].[11,12] However, a small change to the ligand was found to significantly alter the geometry of the phosphorus centers in these compounds: while both **I** and **II** and the analogous diphosphagermylene [{(Trip)$_2$P}$_2$Ge] (**III**) crystallize with one pyramidal and one planar phosphorus center, the corresponding diphosphastannylene [{(Trip)$_2$P}$_2$Sn] (**IV**) crystallizes with two pyramidal phosphorus centers [Trip = 2,4,6-*i*Pr$_3$C$_6$H$_2$].[12] In these compounds the steric bulk of the ligands is associated with the *ortho*-isopropyl groups, since

the *para*-isopropyl groups of the Trip ligands point away from the tetrel centers; it therefore appears that the difference between Dipp and Trip substituents in these compounds, and the consequent preference for a configuration containing two pyramidal phosphorus centers in **IV**, is electronic in origin.

In order to investigate further the impact of the steric and electronic properties of the substituents on the configurations of the phosphorus centers to which they are bound, and thus the stabilization mechanism of the resulting diphosphatetrylenes, we have prepared a series of such compounds possessing two different substituents at each phosphorus center. We report herein the synthesis of these compounds, their solid state structures and their solution behavior, along with a DFT study of the bonding in these species.

Results and Discussion

Treatment of either $GeCl_2$(1,4-dioxane) or $SnCl_2$ with two equivalents of *in situ* generated [(Dipp)(Mes)P]Li(THF)$_3$ (**1Li**)[13] in THF gave the diphosphatetrylenes [(Dipp)(Mes)P]$_2$Ge·(*n*-hexane)$_{0.5}$ (**1Ge**) and [(Dipp)(Mes)P]$_2$Sn (**1Sn**), after crystallization [Mes = 2,4,6-$Me_3C_6H_2$]. In spite of the moderate isolated yields, $^{31}P\{^1H\}$ NMR spectra of the crude solutions indicate that **1Ge** and **1Sn** are essentially the sole phosphorus-containing products from these reactions. The solid-state structure of **1Ge** is shown in Figure 1; with the exception of the solvent of crystallization, **1Sn** is isostructural with **1Ge**.

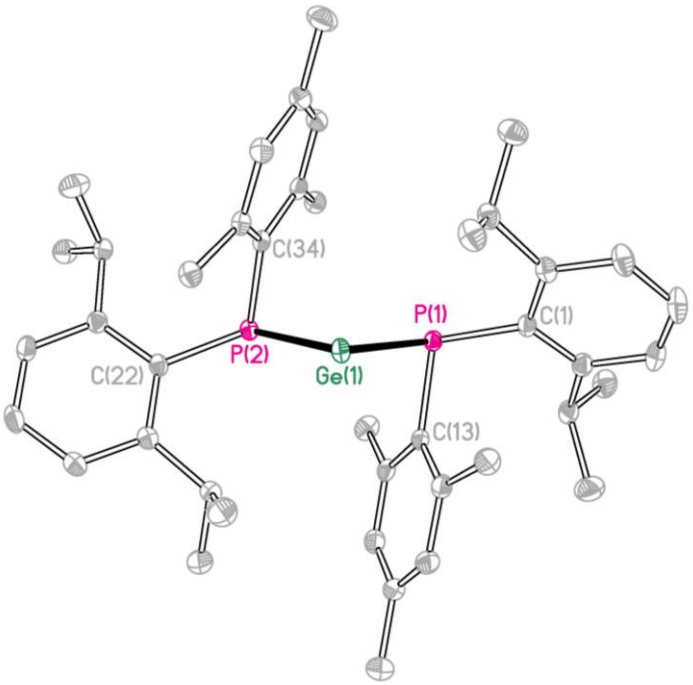

Figure 1. Molecular structure of **1Ge** with 40% probability ellipsoids and with H atoms and solvent of crystallization omitted for clarity. Selected bond lengths (Å) and angles (°) for **1Ge** [values for isostructural **1Sn** in square brackets]: P(1)-E 2.3977(4) [2.5882(4)], P(2)-E 2.3978(4) [2.5847(4)], P(1)-C(1) 1.8588(14) [1.8520(15)], P(1)-C(13) 1.8600(14) [1.8570(15)], P(2)-C(22) 1.8573(14) [1.8515(15)], P(2)-C(34) 1.8613(14) [1.8610(15)], P(1)-E-P(2) 91.873(13) [91.994(12)], C(1)-P(1)-C(13) 104.06(6) [105.58(7)], C(1)-P(1)-E 113.28(5) [108.99(5)], C(13)-P(1)-E 77.61(4) [78.02(5)], C(22)-P(2)-C(34) 106.50(6) 107.53(7)], C(22)-P(2)-E 111.18(5) [110.04(5)], C(34)-P(2)-E 73.12(4) [73.81(5)].

Both **1Ge** and **1Sn** crystallize as discrete monomers with a V-shaped P-E-P core [P(1)-Ge(1)-P(2) 91.873(13), P(1)-Sn(1)-P(2) 91.994(12)°]. The two phosphorus atoms in both **1Ge** and **1Sn** adopt a pyramidal geometry [sum of angles at P = 294.95 and 290.80° (**1Ge**), 292.59 and 291.38° (**1Sn**)] and the P-Ge and P-Sn distances [P(1)-Ge(1) 2.3977(4), P(2)-

Ge(1) 2.3978(4) Å; P(1)-Sn(1) 2.5882(4), P(2)-Sn(1) 2.5874(4) Å] are typical for a P-Ge(II)/Sn(II) σ-bond.[2-9]

Compounds **1Ge** and **1Sn** are chiral at each of the phosphorus centers, crystallizing as a racemic mixture of *RR* and *SS* diastereomers. In each compound, the smaller mesityl substituents occupy the pseudo-axial positions and these groups are significantly canted towards the tetrel atoms, such that the C(*ipso*)-P-Ge/Sn angles are 77.61(4) and 73.12(4)° (**1Ge**) and 78.02(5) and 73.81(5)° (**1Sn**). This leads to short C(*ipso*)···Ge/Sn distances of 2.7008(14) and 2.5736(14) Å (**1Ge**) and 2.855(2) and 2.7315(14) Å (**1Sn**), which are significantly shorter than the sum of van der Waal's radii of the respective elements (sum of radii for C and Ge = 3.8 Å, for C and Sn = 3.95 Å).[14] The acute C(*ipso*)-P-E angles and short C(*ipso*)…E distances suggest a significant interaction between the π-electron density of the mesityl rings and the vacant p-orbital at the tetrel center, which serves to mitigate the electron deficiency of the tetrel center; this is confirmed by DFT calculations (see below). Similar short C(*ipso*)···Ge/Sn contacts have been observed previously in the closely related diarsatetrylenes [{(Dipp)$_2$As}$_2$E] (E = Ge, Sn).[15] In light of these results, we have re-evaluated the structure of the previously reported [{(Trip)$_2$P}$_2$Sn],[12] which also contains two pyramidal phosphorus centers. This reveals a similar, although less pronounced, canting of two of the aromatic rings towards the tin center, resulting in relatively short C(*ipso*)···Sn distances of 2.9813(1) and 2.882(2) Å and acute C(*ipso*)-P-Sn angles of 82.37(7) and 79.20(8)°.

The room temperature ^{1}H and ^{13}C{^{1}H} NMR spectra of **1Ge** are consistent with a single ligand environment. However, at lower temperatures the ^{1}H NMR spectrum of **1Ge** exhibits multiple, overlapping, broad signals, consistent with the presence of more than one species. More information may be gleaned from the variable-temperature ^{31}P{^{1}H} NMR

spectra of **1Ge** (Figure 2). At room temperature the spectrum consists of a relatively sharp singlet at -6.5 ppm (**A**); as the temperature is reduced, this signal broadens and moves to higher field, eventually decoalescing at -60 °C into two signals at -42.9 (**B**) and approximately 12 ppm (**C**), with the latter signal extremely broad. As the temperature is reduced to -90 °C, peak **B** sharpens and peak **C** decoalesces into two, equal, but low intensity, broad singlets at 79.3 (**D**) and -51.6 ppm (**E**). Based on our earlier observations of the achiral diphosphagermylenes **I** and **III**, we attribute this behavior to the operation of two independent equilibria, one of which (***a***) interconverts a configuration with two pyramidal phosphorus centers and a configuration with one pyramidal and one planar phosphorus center, and a second equilibrium (***b***) which interconverts the planar and pyramidal phosphorus centers within the latter configuration (Scheme 1).[16] At room temperature rapid exchange is observed, leading to a time-averaged spectrum, while, at low temperatures signals are observed for the configuration with two pyramidal phosphorus centers (**B**) and for the planar (**D**) and pyramidal (**E**) phosphorus centers of the alternative configuration. From the spectra it is clear that the configuration with two pyramidal phosphorus centers predominates at low temperatures. Similar behavior was observed for compounds **I** and **III**; however, for both of these compounds the low-temperature $^{31}P\{^{1}H\}$ NMR spectra exhibit, in addition to signals corresponding to the configuration with one planar and one pyramidal phosphorus center, two signals which we attributed to different conformations of the configuration with two pyramidal phosphorus centers. We tentatively attribute the presence of a single signal due to the pyramidal/pyramidal form in the low temperature $^{31}P\{^{1}H\}$ NMR spectrum of **1Ge** to the differing sizes of the substituents at the two phosphorus centers, which might favor a single conformation at low temperature.

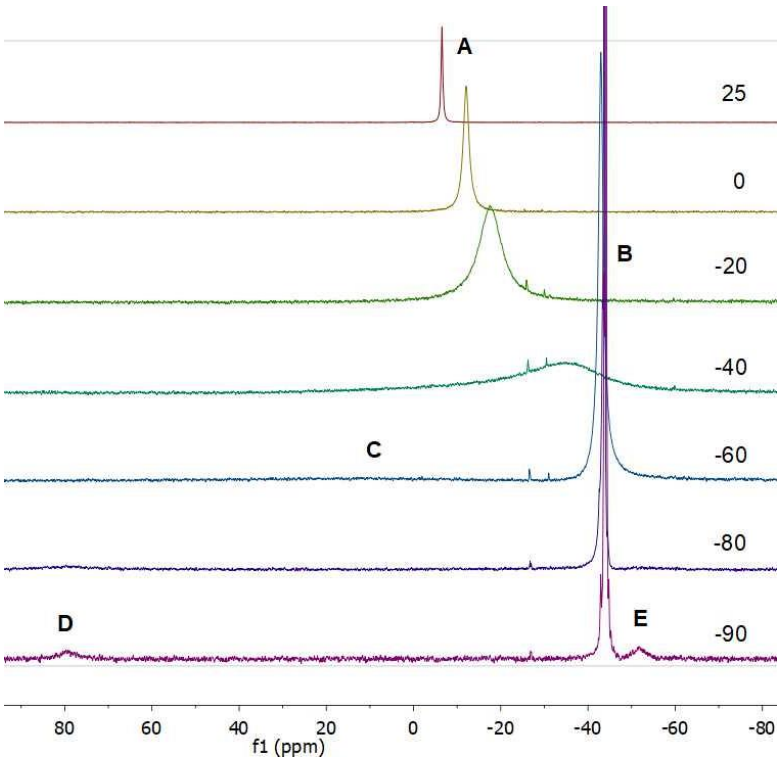

Figure 2. Variable-temperature $^{31}P\{^{1}H\}$ NMR spectra of **1Ge** in d_8-toluene.

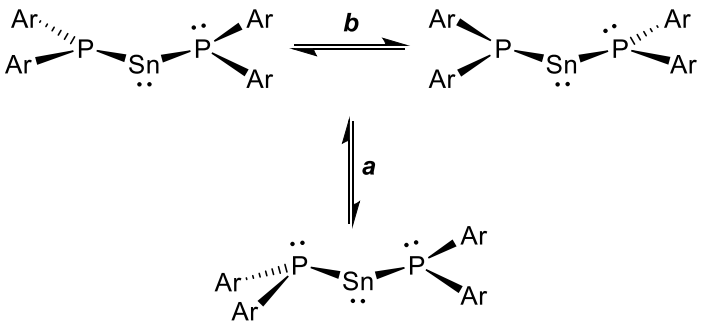

Scheme 1.

The NMR spectra of **1Sn** exhibit rather different behavior. At room temperature the ^{1}H NMR spectrum of **1Sn** (Figure 3) exhibits a single set of signals, consistent with a structure containing two pyramidal phosphorus centers. These signals broaden and decoalesce as the temperature is reduced, until, at -90 °C, the spectrum exhibits four signals due to the CH*Me*$_2$

groups of the Dipp substituents, three signals due to the methyl groups of the mesityl substituents and five signals due to the aromatic protons. We do not attribute this behavior to similar dynamic processes to those observed for **1Ge**, since the $^{31}P\{^{1}H\}$ NMR spectrum of **1Sn** is essentially invariant and the ^{31}P-^{119}Sn coupling constant remains relatively modest over the same temperature range (25 °C: δ_P = -53.5 ppm, J_{PSn} = 850 Hz; -80 °C: δ_P = -59.7 ppm, J_{PSn} = 820 Hz; see the Supporting Information). These latter spectra are consistent with the presence of two pyramidal phosphorus centers over the entire temperature range. In light of this, we attribute the dynamic process responsible for the variable-temperature ^{1}H NMR spectra of **1Sn** to restricted rotation about the P-C(aryl) bonds due to the steric demands of the aryl substituents, such that, at low temperatures, within each (Dipp)(Mes)P ligand each of the *ortho*-methyl groups of the mesityl substituents and each of the methyl and methine groups of the isopropyl moieties of the Dipp substituents are inequivalent. It is also notable that the ^{119}Sn NMR spectrum of **1Sn** consists of a well-resolved triplet at 476 ppm (J_{PSn} = 850 Hz), whereas for **II** and **IV** no ^{119}Sn signal could be observed at room temperature because of the dynamic processes they are subject to and the inherently broad nature of the ^{119}Sn signals in these species.

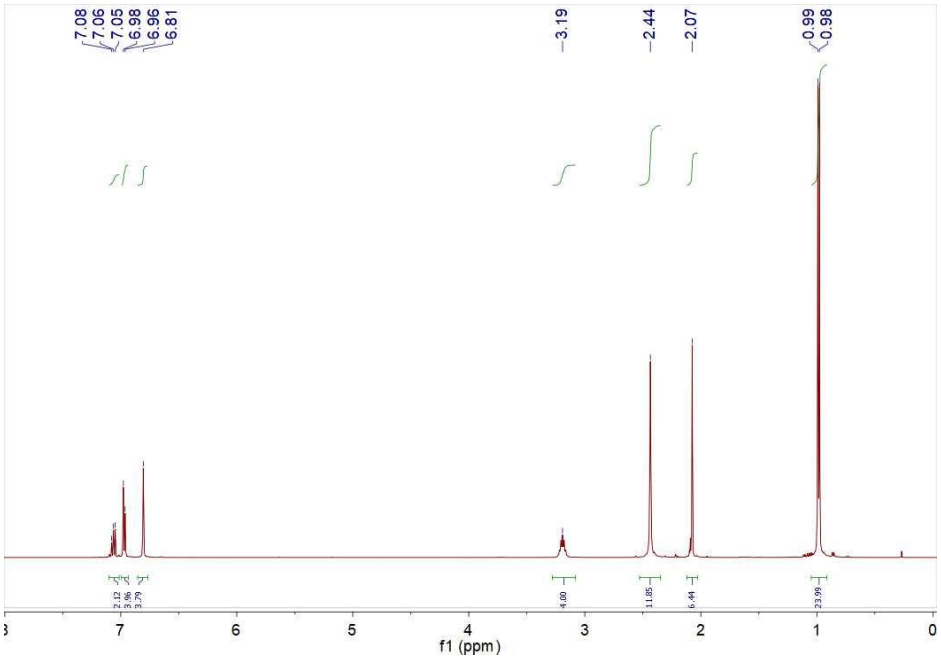

(a)

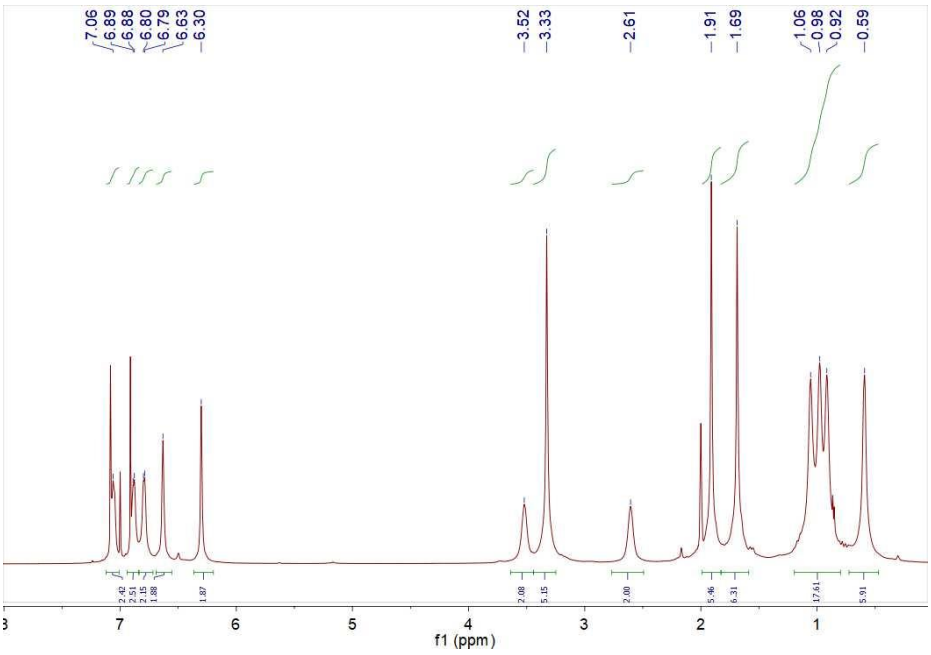

(b)

Figure 3. ^{1}H NMR spectra of **1Sn** at (a) 25 °C and (b) -90 °C.

Thus, we believe that, while **1Ge** exhibits some propensity for planarization at one of the phosphorus centers, this is not the case for **1Sn**. This is counter to previous reports that the barrier to inversion at phosphorus is lower when coordinated to tin compared to the less electronegative germanium or silicon,[17] but is consistent with our DFT calculations (see below). The behavior of **1Sn** also contrasts with the behavior of **II** and **IV** in solution, which show clear evidence for a dynamic equilibrium involving a planar phosphorus center. However, even for **1Ge** it appears that the relative concentration of the planar/pyramidal form is very low. This suggests that the propensity of diphosphatetrylenes to adopt a configuration with a planar phosphorus center is at least partially dependent upon the steric demands of the substituents at phosphorus, with greater steric bulk favoring a planar configuration. In order to explore this hypothesis further, we set out to synthesize the bulkier alkyl/aryl-substituted

tetrylenes [{(Me$_3$Si)$_2$CH}(Dipp)P]$_2$E [E = Ge (**2Ge**), Sn (**2Sn**)] and the peralkyl-substituted [[{(Me$_3$Si)$_2$CH}$_2$P]$_2$E] [E = Ge (**3Ge**), Sn (**3Sn**)] (we note, however, that replacing an aryl group with a silicon-substituted alkyl group is likely also to have an effect on the electronic properties of the phosphorus centers). Compounds **2Ge**/**Sn** should be more hindered than **1Ge** and **1Sn**, whilst still retaining an aryl group which may participate in stabilizing C(*ipso*)···E contacts, while **3Ge**/**Sn** have very bulky substituents which do not permit alternative stabilization mechanisms other than planarization at phosphorus. The steric properties of the ligands may be quantified using the concept of the percent buried volume (%V_{bur}), which is defined as the percentage of a sphere of radius 3.5 Å around the metal centre that is occupied by a given ligand;[18] for comparison, the %V_{bur} for the two ligands (Dipp)(Mes)P and {(Me$_3$Si)$_2$CH}(Dipp)P are 69.0 and 76.8, respectively.

The reaction between {(Me$_3$Si)$_2$CH}PCl$_2$[19] and one equivalent of DippLi(OEt$_2$),[11,20] followed by one equivalent of LiAlH$_4$ gave the secondary phosphine {(Me$_3$Si)$_2$CH}(Dipp)PH (**2H**) in excellent yield as a colorless oil. Treatment of **2H** with *n*BuLi in THF at -78 °C, followed by warming to room temperature and crystallization from a mixture of diethyl ether and light petroleum gave [{(Me$_3$Si)$_2$CH}(Dipp)P]Li(THF)$_3$ (**2Li**) in good yield as yellow blocks. Compound **2Li** crystallizes as discrete monomers in which the lithium ion is coordinated by the phosphorus atom of the ligand and three molecules of THF in a distorted tetrahedral geometry (Figure 4). The structure of **2Li** is typical of sterically hindered lithium phosphides, such as the closely related [{(Dipp)$_2$P}Li(THF)$_3$].[13,21]

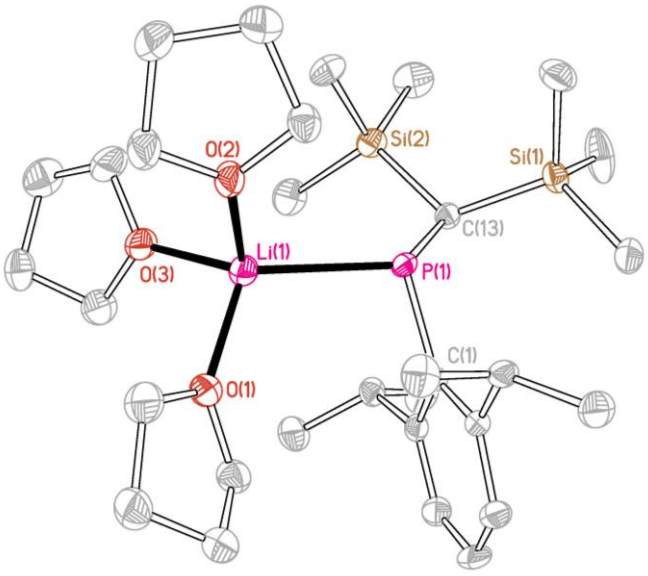

Figure 4. Molecular structure of **2Li** with H atoms omitted for clarity. Selected bond lengths (Å) and angles (deg.): P(1)-Li(1) 2.563(4), P(1)-C(1) 1.851(2), P(1)-C(13) 1.909(2), Li(1)-O(1) 2.000(4), Li(1)-O(2) 1.982(4), Li(1)-O(3) 1.990(4), Li(1)-P(1)-C(1) 103.86(11), Li(1)-P(1)-C(13) 127.90(11), C(1)-P(1)-C(13) 105.24(10).

The room temperature ^{1}H and ^{13}C{^{1}H} NMR spectra of **2Li** are rather broad, but are consistent with the solid-state structure. However, the ^{31}P{^{1}H} and ^{7}Li NMR spectra of **2Li** (Figure 5) indicate a dynamic exchange process to be operative in solution. At room temperature the ^{31}P{^{1}H} NMR spectrum of **2Li** in d_8-toluene exhibits a single broad signal at -117.9 ppm (**F**). As the temperature is reduced this signal broadens further until, at -20 °C, it decoalesces into a 1:1:1:1 quartet at -116.9 ppm (**G**, J_{PLi} = 82 Hz) and a rather broad multiplet at -127.2 ppm (**H**) in an approximate 11:1 ratio. As the temperature is reduced further, signal **G** sharpens and signal **H** decreases in intensity, until, at -80 °C, it is barely resolved. The room temperature ^{7}Li NMR spectrum of **2Li** exhibits a single singlet at 1.2 ppm (**J**) and this broadens and decoalesces as the temperature is reduced such that, at -20 °C, the spectrum consists of a sharp doublet (**K**, J_{PLi} = 82 Hz) and a very broad, low intensity triplet (**L**, J_{PLi} =

67 Hz) in an approximate 1:10 ratio. The foregoing is consistent with a dynamic equilibrium between a monomer and a dimer or higher oligomer containing a P_2Li_2 unit, in which the monomer is favored at low temperatures.

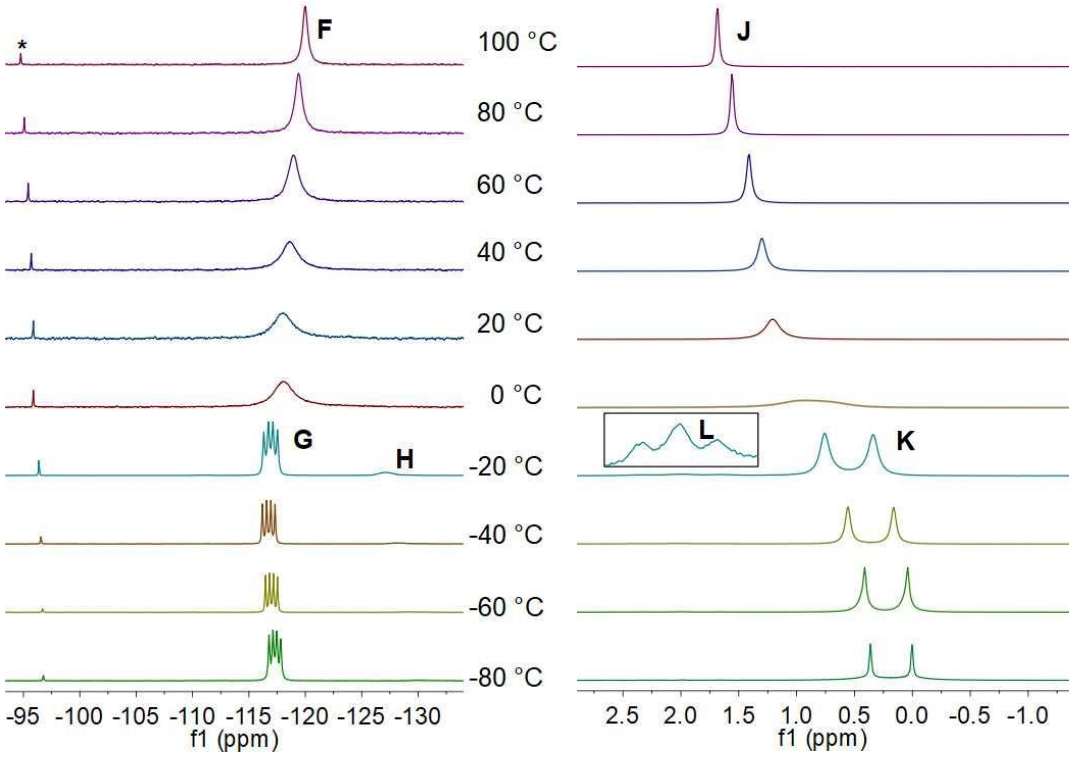

(a) (b)

Figure 5. Variable-temperature (a) $^{31}P\{^1H\}$ and (b) ^7Li NMR spectra of **2Li** in d_8-toluene (*free phosphine **2H**).

The reaction between two equivalents of **2Li** and one equivalent of $SnCl_2$ gave the corresponding diphosphastannylene $[\{(Me_3Si)_2CH\}(Dipp)P]_2Sn$ (**2Sn**) as dark green prisms after crystallization from cold toluene. The corresponding reaction between **2Li** and $GeCl_2$(1,4-dioxane) gave a dark red solution which exhibited a broad singlet in its $^{31}P\{^1H\}$ NMR spectrum at 23.9 ppm, consistent with the formation of a diphosphagermylene;

however, we were unable to obtain a solid sample of this compound due to its very high solubility in even the most non-polar solvents such as hexane or hexamethyldisiloxane.

Compound **2Sn** crystallizes as a V-shaped monomer with a P-Sn-P angle of 91.548(15)° (Figure 6). Like **1Ge** and **1Sn**, compound **2Sn** crystallizes with two pyramidal phosphorus centers and is thus chiral at each of these, crystallizing as the *rac* diastereomer in which the two Dipp groups occupy the pseudo-axial positions. The P-Sn distances [2.5726(5) and 2.5810(5) Å] and the P-Sn-P angle are similar to those observed for **1Sn**. In **2Sn** only one of the two aromatic rings is significantly canted towards the tin atom, such that the C(*ipso*)-P-Sn angle is 78.75(6)° (the second Dipp group lies further from the tin center, with a C(*ipso*)-P-Sn angle of 95.56(6)°). This leads to a relatively short C(*ipso*)···Sn distance of 2.877(2) Å, once again suggesting substantial delocalization of the aromatic π-electron density into the vacant 5p orbital at tin. The presence of a single C(*ipso*)···Sn contact in **2Sn**, rather than the two interactions observed for each of **1Ge** and **1Sn** is attributed to the increased steric bulk of the phosphide ligand in **2Sn**.

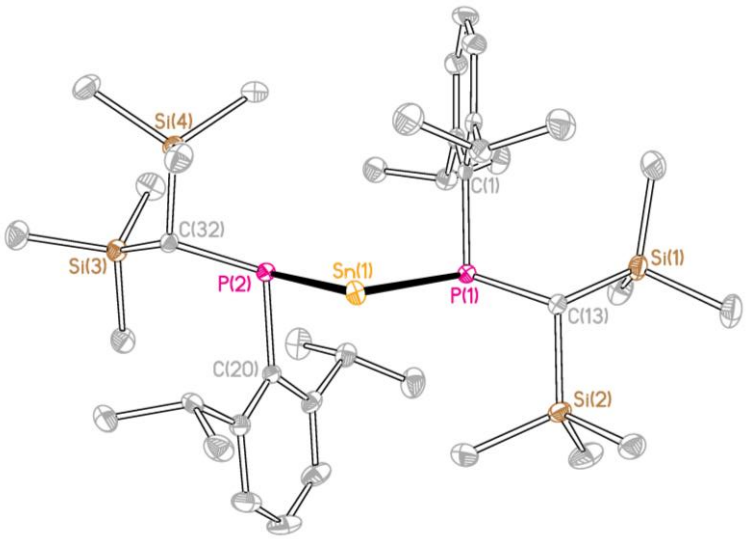

Figure 6. Molecular structure of **2Sn** with H atoms omitted for clarity. Selected bond lengths (Å) and angles (°): P(1)-Sn(1) 2.5726(5), P(2)-Sn(1) 2.5810(5), P(1)-C(1) 1.8711(19),

P(1)-C(13) 1.8778(18), P(2)-C(20) 1.8716(19), P(2)-C(32) 1.8792(18), P(1)-Sn(1)-P(2) 91.548(15), C(1)-P(1)-C(13) 106.56(8), C(1)-P(1)-Sn(1) 95.56(8), C(13)-P(1)-Sn(1) 108.51(6), C(20)-P(2)-C(32) 109.45(8), C(20)-P(2)-Sn(1) 78.75(6), C(32)-P(2)-Sn(1) 114.30(6).

In contrast to **1Sn**, the solution behavior of **2Sn** closely resembles that of **II** and **IV**. The room temperature $^{31}P\{^{1}H\}$ NMR spectrum of **2Sn** in d_8-toluene (see Supporting Information) consists of a broad singlet at -30.2 ppm exhibiting tin satellites (J_{PSn} = 1030 Hz). As the temperature is reduced, this signal begins to broaden and move to higher field, such that, at -20 °C, the spectrum consists of a very broad singlet at -35.0 ppm (fwhm ca 300 Hz). This signal then begins to sharpen as the temperature is reduced further until, at -90 °C, the spectrum consists of a reasonably sharp singlet at -39.4 ppm exhibiting tin satellites (J_{PSn} = 920 Hz). The increasingly negative chemical shift and smaller ^{31}P-$^{117/119}Sn$ coupling constant observed as the temperature is reduced, suggest a dynamic equilibrium between a configuration containing two pyramidal phosphorus centers and one containing one planar and one pyramidal phosphorus center, of which the former predominates, especially at lower temperatures.

In 1984 Lappert and co-workers reported that the reaction between two equivalents of $[\{(Me_3Si)_2CH\}_2P]Li$ (**3Li**) and $SnCl_2$ in diethyl ether at room temperature did not give the corresponding diphosphastannylene; instead, **3Li** acted as a reducing agent to give elemental tin and the persistent phosphinyl radical $\{(Me_3Si)_2CH\}_2P^{\cdot}$.[22] We have now found that the reaction between two equivalents of **3Li** and $SnCl_2$ in THF *at -78 °C* yields a red solution containing dark solids, which we presume to be elemental tin. However, filtration and removal of solvent from the filtrate yields a sticky red solid, from which dark red crystals of

the diphosphastannylene [{$(Me_3Si)_2CH$}$_2$P]$_2$Sn (**3Sn**) spontaneously crystallize. Unfortunately, due to the manner of isolation and the extremely soluble nature of this compound (even in non-polar solvents such as hexane or hexamethyldisiloxane), only a very small number of crystals of **3Sn** were isolated from this reaction and insufficient material was available for full characterization. Nonetheless, we were able to obtain a crystal structure of **3Sn**. This shows that **3Sn** crystallizes as a discrete V-shaped monomer [P-Sn-P 101.614(18)°], with one pyramidal and one planar phosphorus center [sum of angles at P(1) = 359.52, P(2) = 311.98°] (Figure 7).

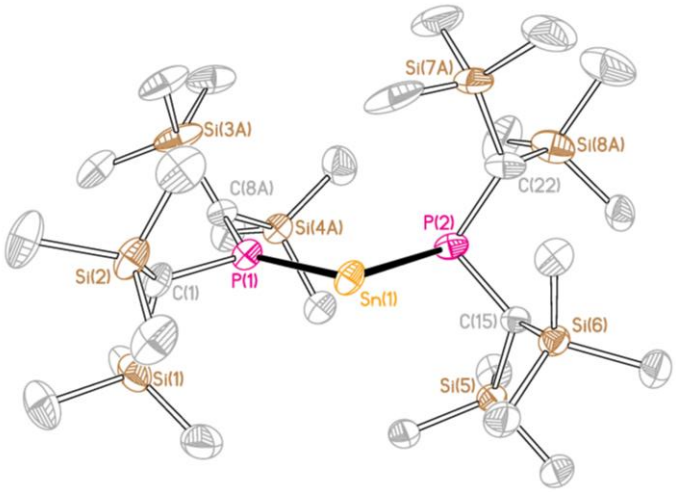

Figure 7. Molecular structure of **3Sn** with H atoms and minor disorder components omitted for clarity. Selected bond lengths (Å) and angles (°): P(1)-Sn(1) 2.4287(5), P(2)-Sn(1) 2.6226(5), P(1)-C(1) 1.854(2), P(1)-C(8A) 1.866(6), P(2)-C(15) 1.894(2), P(2)-C(22) 1.891(2), P(1)-Sn(1)-P(2) 101.614(18), C(1)-P(1)-C(8A) 101.7(2), C(1)-P(1)-Sn(1) 114.34(7), C(8A)-P(1)-Sn(1) 143.48(19), C(15)-P(2)-C(22) 100.99(11), C(15)-P(2)-Sn(1) 97.80(6), C(22)-P(2)-Sn(1) 113.19(8).

The P(1)-Sn(1) distance of 2.4287(5) Å is approximately 0.16 Å, or 7%, shorter than the P(2)-Sn(1) distance of 2.5810(5) Å, consistent with substantial multiple bond character in

the former. However, it should be noted that a portion of the decrease in the P-Sn distances on going from a pyramidal to a planar phosphorus center may be attributed to the change in hybridization of the phosphorus atom from sp^3 to sp^2; this effect has been described previously for a series of boryl-substituted phosphorus compounds in which there is the potential for a similar P=B π-interaction.[23]

While we were unable to obtain sufficient material for a full characterization of **3Sn**, a $^{31}P\{^1H\}$ NMR spectrum of the crude reaction mixture indicates that **3Sn** is the dominant diamagnetic phosphorus-containing material (see the Supporting Information). The spectrum consists of a singlet at 43.2 ppm exhibiting tin satellites (J_{PSn} = 1900 Hz). The relatively low-field chemical shift and large ^{31}P-$^{117/119}Sn$ coupling constant of this compound strongly suggest that there is a large component of the planar/pyramidal configuration at room temperature (see above); this is supported by DFT calculations (see below).

We also attempted the reaction between two equivalents of **3Li** and one equivalent of $GeCl_2$(1,4-dioxane). However, while a $^{31}P\{^1H\}$ NMR spectrum of the dark red, crude reaction mixture exhibited a broad singlet at 49.9 ppm, consistent with the formation of the corresponding diphosphagermylene $[\{(Me_3Si)_2CH\}_2P]_2Ge$, we were unable to isolate this material in the solid state, due to its high solubility in non-polar solvents, and so were unable to undertake further characterization.

In order to gain insight into the relative stabilities of the different configurations of **1Ge**, **1Sn**, **2Sn** and **3Sn** and to further probe the relative stabilizing effects of the P-E π-interactions and arene…E contacts, we have carried out a DFT study of these molecules. Each of **1Ge**, **1Sn** and **2Sn** possesses two different substituents at each phosphorus center, and so, for the geometries containing a planar phosphorus atom, four potential stereoisomers are possible. In these isomers the planar phosphorus center may have either substituent *syn* to the second phosphorus lone pair, while the pyramidal phosphorus center may have either *R* or

S stereochemistry (Figure 8). For the geometries of **1Ge**, **1Sn** and **2Sn** containing two pyramidal phosphorus centers, both *rac*- and *meso*-diastereomers are possible and, for each of the *rac* isomers, either substituent may occupy the pseudo-axial positions.

For **1Ge** our DFT calculations reveal a rather shallow potential energy surface. The geometry corresponding to that found by X-ray crystallography [**1Ge(pyr_a1)**] is more stable than the majority of alternative geometries by between 1.0 and 11.4 kJ mol^{-1}, with only **1Ge(plan_a1)** lying to significantly higher free energy (20.9 kJ mol^{-1}; Figure 9). However, the most stable geometry of **1Ge** is derived from a starting configuration corresponding to **1Ge(plan_a2)**, but which converges to a geometry containing two near-planar phosphorus centers (see Supporting Information); even this latter geometry is more stable than **1Ge(pyr_a1)** by just 7.1 kJ mol^{-1}. The foregoing is consistent with the operation of a dynamic equilibrium in solution which interconverts the planar/pyramidal and pyramidal/pyramidal forms, as observed by variable temperature $^{31}P\{^{1}H\}$ NMR spectroscopy (see above). The preference for a geometry corresponding to **1Ge(pyr_a1)** in the solid state is also consistent with the above, since the difference in free energy between the majority of conformations is rather small and since crystal packing effects may be significant.

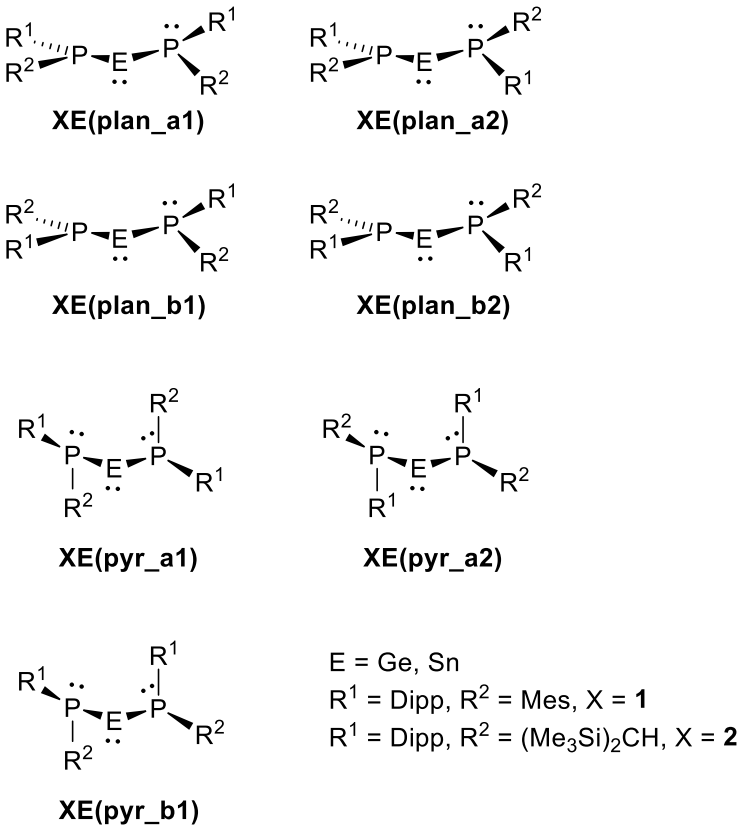

Figure 8. Possible geometries for **1Ge**, **1Sn** and **2Sn**.

For **1Sn** the most stable geometry [**1Sn(pyr_a1)**] corresponds to that observed in the solid state. While the alternative geometries containing two pyramidal phosphorus centers are close in energy to **1Sn(pyr_a1)**, the geometries containing a planar phosphorus center lie between 24.0 and 39.1 kJ mol^{-1} higher in free energy. This is consistent with the preference of **1Sn** for a geometry corresponding to **1Sn(pyr_a1)** in the solid state and the preference for a structure containing two pyramidal phosphorus centers in solution, as observed by variable temperature $^{31}P\{^{1}H\}$ NMR spectroscopy.

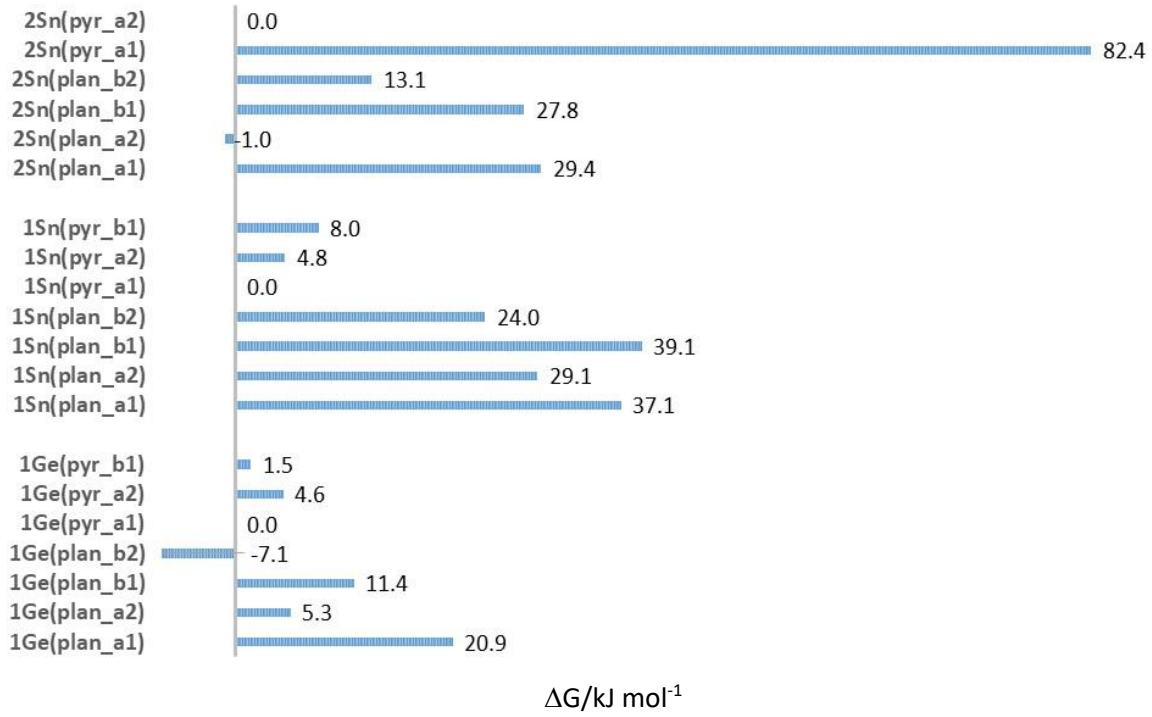

Figure 9. Relative free energies of the calculated geometries of **1Ge**, **1Sn**, and **2Sn** (values in kJ mol^{-1} are relative to the geometry corresponding to the solid sate structure in each case).

For **2Sn** geometries **2Sn(pyr_a2)**, corresponding to the structure observed in the solid state, and **2Sn(plan_a2)** are essentially isoergonic. The remaining geometries are significantly higher in free energy (we were unable to locate a stable minimum energy geometry corresponding to **2Sn(pyr_b1)**, possibly due to steric effects). The similar free energies of **2Sn(pyr_a2)** and **2Sn(plan_a2)** are again consistent with the variable temperature $^{31}P\{^{1}H\}$ NMR spectra of **2Sn**, which indicate a rapid dynamic equilibrium between a form containing two pyramidal phosphorus centers and a second form containing one pyramidal and one planar phosphorus center.

In contrast to the above, DFT calculations on **3Sn** show a strong energetic preference (52.4 kJ mol^{-1}) for the form containing one planar and one pyramidal phosphorus center.

Natural Bond Orbital (NBO) analysis of the configurations of **1Ge** containing a planar phosphorus center [**1Ge(plan_x**)] indicate that the Ge-P(planar) interactions may be described as consisting of a σ- and a π-bond. The Ge-P(planar) bonds have Wiberg Bond Indices (WBIs) of 1.275-1.346, consistent with significant multiple bond character (see the Supporting Information, Table S2). These contrast with the purely σ-bonded Ge-P(pyramidal) bonds, which have WBIs in the range 0.875-0.933. The exception to this is provided by **1Ge(plan_b2)**, which converges to a geometry in which the two phosphorus centers approach a planar configuration [sum of angles at P = 354.01 and 354.58°] and which has WBIs for the Ge-P bonds of 1.171 and 1.170.

NBO analyses also reveal that geometries **1Ge(plan_a1)**, **1Ge(plan_a2)**, and **1Ge(plan_b1)** are additionally stabilized by delocalization of the largely *s*-character lone pair at germanium into the σ*-orbital of the C-P(planar) bond which is directed towards the rear of the molecule, resulting in an unusual push-pull stabilization of the diphosphagermylene. For such delocalizations the E(2) energy, calculated from second order perturbation theory analysis, provides an approximate measure of the stabilization afforded by each delocalization; for the Ge(lone pair)→P-C(σ*) delocalizations in **1Ge(plan_x)** the E(2) energies range from 33.4 to 51.5 kJ mol^{-1}.

For the minimum energy geometries of **1Ge** containing two pyramidal phosphorus centers [**1Ge(pyr_x)**] the calculated WBIs for the Ge-P bonds range from 0.738-0.765, consistent with a single bond in each case. The close approach of one or more of the aromatic rings in these geometries is reflected in WBIs for the Ge···C(*ipso*) interactions which are significantly greater than zero [typically around 0.1]. In support of this apparent weak bonding interaction, NBO analyses indicate substantial delocalization of electron density from the aromatic rings into the formally vacant 4p orbital on germanium, resulting in

occupation of this orbital by approximately 0.2 of an electron. For **1Ge(pyr_x)** the sums of the pertinent E(2) energies for the aryl···Ge delocalizations range from 218.5 to 232.3 kJ mol^{-1} (see Table S2 in the Supporting Information).

A similar situation is found for **1Sn**, although, in three of the four possible geometries containing a "planar" phosphorus center, this atom is somewhat more pyramidal than is observed in **1Ge** [sum of angles at "planar" P = 341.89, 346.62, 353.43, and 359.84°]. According to the NBO analyses, the bonding in these geometries is best described as arising from a P-Sn σ-bond, supplemented by partial delocalization of electron density from the phosphorus lone pair into the vacant 5p-orbital at tin, rather than a true σ+π bond. This results in a weaker Sn-P interaction, with WBIs ranging from 0.956-1.144, compared to WBIs of 0.757-0.876 for the second, purely σ-type, Sn-P(pyramidal) bond. The P-Sn π-interaction results in occupation of the formally vacant tin 5p orbital by between 0.38 and 0.40 of an electron. Once again, stabilization due to the P-Sn π-interaction is supplemented by delocalization of the tin lone pair into a P-C σ*-orbital at the planar phosphorus center [range of E(2) energies 7.5-43.5 kJ mol^{-1}].

For the geometries of **1Sn** containing two pyramidal phosphorus centers NBO analyses indicate some delocalization of the electron density from the adjacent aromatic rings, although this is somewhat less than was found for the similar geometries of **1Ge** [the sums of the pertinent E(2) energies for the aryl…Sn delocalizations range from 147.3 to 163.6 kJ mol^{-1}]. These delocalizations result in population of the formally vacant 5p orbital by between 0.16 and 0.17 of an electron.

The planar phosphorus centers in the minimum energy geometries **2Sn(plan_x)** are significantly more planar than in the majority of the corresponding geometries of **1Sn** [range of the sum of angles at planar P = 353.88-357.56° for **2Sn**], leading to more substantial

delocalization of the phosphorus lone pairs from the planar phosphorus atoms into the formally vacant 5p-orbital on tin. This leads to population of the 5p-orbitals by between 0.37 and 0.40 of an electron and WBIs for these bonds of between 1.199 and 1.232. The increased planarity of these phosphorus atoms and the consequent increase in the P-Sn multiple bond character may be attributed, at least in part, to the greater steric bulk of the $(Me_3Si)_2CH$ group in comparison to a mesityl substituent, which enforces greater R-P-Ar angles. Of the two configurations of **2Sn** containing two pyramidal phosphorus centers, only one, **2Sn(pyr_a2)** is able to form C(aryl)…Sn contacts. However, for this form, which corresponds to the solid-state structure, only one of the aryl rings appears to be canted towards the tin center [C(aryl)-P-Sn angles 83.79 and 96.84°], and even this is considerably less than that observed in the corresponding minimum energy geometries of **1Sn** and **1Ge**, suggesting significantly reduced stabilization via this mechanism. This is confirmed by the low value for the sum of E(2) energies for the delocalization of electron density from this aromatic ring into the formally vacant 5p orbital at tin [sum of pertinent E(2) energies = 40.1 kJ mol^{-1}].

For the geometry of **3Sn** containing a planar phosphorus center, **3Sn(plan)**, the Sn-P(planar) bond has a WBI of 1.281, while the Sn-P(pyramidal) bond has a WBI of 0.794, suggesting substantial multiple bond character in the former. Indeed, NBO analysis suggests that this bond is best described as being comprised of a true $\sigma+\pi$ combination. Stabilization by this π-interaction is supplemented by delocalization of the tin lone pair into one of the P-C σ^*-orbitals [E(2) energy 28.2 kJ mol^{-1}], again suggesting an unusual push-pull stabilization mechanism. For the geometry of **3Sn** containing two pyramidal phosphorus centers, **3Sn(pyr)**, the Sn-P WBIs are 0.838 and 0.819, consistent with single bonds. Since **3Sn** has no aromatic substituents, opportunities for further stabilization of **3Sn(pyr)** are limited, consistent with the high relative free energy of **3Sn(pyr)** in comparison to **3Sn(plan)**; however, two of the methyl hydrogen atoms in **3Sn(pyr)** lie in close proximity to the tin

center and NBO analysis indicates that there is delocalization of the C-H σ-bonding electron density into the formally vacant tin 5p-orbital, with E(2) energies for these delocalizations of 28.2 and 17.7 kJ mol^{-1}.

Conclusions:

Monomeric diphosphatetrylenes may adopt a configuration possessing either two pyramidal phosphorus centers or one planar and one pyramidal phosphorus center. The present study suggests that the preference for one or other of these configurations is determined by a delicate balance between (i) the strength of the potential P=E π-interaction, (ii) the potential for arene…E interactions, (iii) the barrier to planarization at phosphorus, and (iv) the steric demands of the substituents. Sterically bulky substituents (e.g. Dipp, $(Me_3Si)_2CH$) tend to favor a planar phosphorus geometry (e.g. **I**, **II**, **III**, **3Sn**)), while the presence of aromatic substituents enables arene…E interactions which can compete with any potential P=E π-interactions (e.g. **1Ge**, **1Sn**, **2Sn**).

For **1Ge** these factors are finely balanced, such that there is no strong preference for either configuration: in the solid state **1Ge** crystallizes with two pyramidal phosphorus centers, whereas in solution a dynamic equilibrium between this form and a configuration containing one planar and one pyramidal phosphorus center operates. In support of this, DFT calculations indicate a very shallow potential energy surface. Compound **1Ge** is very similar to **I**/**III** but has one Dipp group on each phosphorus atom replaced by a smaller Mes substituent. The difference in structural preference may, therefore, be attributed to the greater steric bulk around the phosphorus centers in **I** and **III**, which enforces greater Ar-P-Ar and Ar-P-Ge angles and so lowers the barrier to planarization at the phosphorus center, favoring a configuration with one planar and one pyramidal phosphorus atom in these compounds.

For **1Sn** there is a strong preference for a configuration possessing two pyramidal phosphorus centers, both in the solid state and solution. While it may be expected that the presence of a more electropositive tin atom adjacent to phosphorus might lower the barrier to planarization of the latter center, it appears that the lower steric bulk of the ligands in **1Sn**, coupled with the poorer P=Sn π-overlap in the planar configuration and the strong arene…Sn interactions in the pyramidal form, significantly favor the latter configuration.

For **2Sn** there is again no strong preference for a particular configuration, with the minimum energy configuration, which possesses a planar phosphorus center, being essentially isoergonic with a form containing two pyramidal phosphorus centers. In this case, only one significant arene…Sn interaction is observed in the form containing two pyramidal phosphorus centers, making the configuration with a planar phosphorus center more competitive.

Finally, in contrast to the above, **3Sn** exhibits a very strong preference for the configuration with one planar and one pyramidal phosphorus center. This may be attributed to the very bulky substituents at phosphorus and the absence of competing arene…Sn interactions in the configuration possessing two pyramidal phosphorus centers.

Overall, we conclude that, while P=E π-interactions can significantly stabilize diphosphatetrylenes, they are not necessarily essential and are competitive with arene…E interactions in these compounds.

Experimental Procedure:

General: All manipulations were carried out using standard Schlenk and dry-box techniques under an atmosphere of dry nitrogen or argon. THF, diethyl ether, toluene, *n*-hexane, methylcyclohexane and light petroleum (b.p. 40-60°C) were dried prior to use by distillation under nitrogen from sodium, potassium, or sodium/potassium alloy, as

appropriate. THF was stored over activated 4A molecular sieves; all other solvents were stored over a potassium film. Deuterated toluene was distilled from potassium and $CDCl_3$ was distilled from CaH_2 under argon; all NMR solvents were deoxygenated by three freeze-pump-thaw cycles and were stored over activated 4A molecular sieves. $DippLi(OEt_2)$,[20] (Mes)(Dipp)PH,[13] and $\{(Me_3Si)_2CH\}PCl_2$[19] were prepared according to previously published procedures. *n*-Butyllithium was purchased from Aldrich as a 2.5 M solution in hexanes and its concentration accurately determined by titration before use. All other compounds were used as supplied by the manufacturer.

^1H and $^{13}C\{^1H\}$ NMR spectra were recorded on a Bruker AvanceIII 500 spectrometer operating at 500.16 and 125.65 MHz, respectively, or a Bruker AvanceIII 300 spectrometer operating at 300.15 and 75.47 MHz, respectively; chemical shifts are quoted in ppm relative to tetramethylsilane. ^7Li, $^{31}P\{^1H\}$ and $^{119}Sn\{^1H\}$ NMR spectra were recorded on a Bruker AvanceIII 500 spectrometer operating at 194.38, 202.35 and 186.59 MHz, respectively; chemical shifts are quoted in ppm relative to external 0.1 M LiCl, 85% H_3PO_4 and Me_4Sn, respectively.

Due to the air- and moisture-sensitive nature of the reported compounds, satisfactory elemental analyses could not be obtained; however, bulk purity is confirmed by multinuclear NMR spectroscopy for each compound (see the Supporting Information).

Synthesis of (Dipp){(Me$_3$Si)$_2$CH}PH (2H): To a cold (-10 °C) solution of $\{(Me_3Si)_2CH\}PCl_2$ (3.08 g, 11.8 mmol) in diethyl ether (50 mL) was added, dropwise, a solution of $DippLi(OEt_2)$ (2.85 g, 11.8 mmol) in diethyl ether (20 mL). The resulting pale yellow solution containing pale solids was allowed to warm to room temperature and was stirred for 1 h. The mixture was cooled to 0 °C and solid $LiAlH_4$ (0.44 g, 11.7 mmol) was added in portions. This mixture was allowed to warm to room temperature and was stirred for 1 h. The mixture was cooled to 0 °C and degassed water (50 mL) was added slowly. The

product was extracted into light petroleum (3 x 15 mL) and the combined organic phases were dried over 4 Å molecular sieves. The solution was filtered and the solvent was removed from the filtrate under vacuum to give a pale yellow oil. Impurities were removed by vacuum distillation (100 °C/ 1 x 10^{-3} Torr) to leave the product as a pale yellow oil. Yield: 3.33 g, 80%. ^{1}H NMR [$CDCl_3$, 298 K]: δ -0.02 (s, 9H, CH(*SiMe*$_3$)(SiMe$_3$)), 0.11 (s, 9H, CH(SiMe$_3$)(*SiMe*$_3$)), 0.60 (d, J_{HH} = 5.8 Hz, 1H, C*H*(SiMe$_3$)(SiMe$_3$)), 1.25 (d, J_{HH} = 6.8 Hz, 6H, CH*Me*Me), 1.26 (d, J_{HH} = 6.8 Hz, 6H, CHMe*Me*), 3.76 (m, 2H, C*H*MeMe), 4.40 (dd, J_{PH} = 218.5 Hz, J_{HH} = 5.8 Hz, 1H, PH), 7.11 (d, J_{HH} = 7.6 Hz, 1H, ArH), 7.12 (d, J_{HH} = 7.6 Hz, 1H, ArH), 7.29 (t, J_{HH} = 7.6 Hz, 1H, ArH). ^{13}C{^{1}H} NMR [$CDCl_3$, 298 K]: δ 1.00 (d, J_{PC} = 3.6 Hz, CH(SiMe$_3$)(*SiMe*$_3$)), 1.30 (d, J_{PC} = 6.2 Hz, CH(*SiMe*$_3$)(SiMe$_3$)), 9.20 (d, J_{PC} = 47.2, C*H*(SiMe$_3$)(SiMe$_3$)), 24.18 (CH*Me*Me), 25.27 (CHMe*Me*), 32.72 (d, J_{PC} = 14.4, *C*HMeMe), 123.30 (d, J_{PC} = 3.1 Hz, Ar), 129.39 (Ar), 133.38 (d, J_{PC} = 24.0 Hz, Ar), 153.72 (d, J_{PC} = 12.1 Hz, Ar). ^{31}P NMR [$CDCl_3$, 298 K]: δ -96.0 (d, J_{PH} = 218.5 Hz).

Synthesis of [(Dipp){(Me$_3$Si)$_2$CH}P]Li(THF)$_3$ (2Li): To a cold (-78 °C) solution of (Dipp){(Me$_3$Si)$_2$CH}PH (0.75 g, 2.13 mmol) in THF (10 mL) was added a solution of *n*BuLi in hexanes (2.3 M, 0.9 mL, 2.07 mmol) and this mixture was allowed to warm to room temperature. The resulting red solution was stirred for 30 min and the solvent was removed *in vacuo*. The sticky orange solid was dissolved in a mixture of diethyl ether (5 mL) and light petroleum (5 mL) and this solution was stored at -25 °C overnight, yielding large orange crystals of **2Li**. The supernatant was removed by filtration, the orange crystals were washed with cold (0 °C) light petroleum (10 mL) and residual solvent was removed under vacuum. Yield: 0.50 g, 41%. ^{1}H NMR [d_8-toluene, 253 K]: δ 0.42 (s, 18H, CH(*SiMe*$_3$)$_2$), 0.93 (s, 1H, C*H*(SiMe$_3$)$_2$), 1.32 (m, 12H, THF), 1.48 (d, J_{HH} = 6.6 Hz, 12H, CH*Me*$_2$), 3.36 (br. m, 12H, THF), 4.94 (br. s, 2H, C*H*Me$_2$), 7.18 (m, 3H, ArH). ^{13}C{^{1}H} NMR [d_8-toluene, 253 K]: δ 1.87 (d, J_{PC} = 5.4 Hz, CH(*SiMe*$_3$)$_2$), 8.08 (J_{PC} = 66.3 Hz, *C*H(SiMe$_3$)$_2$), 25.29 (THF), 25.58

(CH*Me*$_2$), 32.86 (d, J_{PC} = 15.1 Hz, *C*HMe$_2$), 68.12 (THF), 122.03, 122.95, 152.21 (Ar), 153.63 (d, J_{PC} = 57.5 Hz, Ar). ^{7}Li NMR [d_8-toluene, 253 K]: 2.0 (t, J_{LiP} = 67 Hz), 0.5 (d, J_{LiP} = 82 Hz) in a 1:10 ratio. ^{31}P{^{1}H} NMR [d_8-toluene, 253 K]: -116.9 (q, J_{LiP} = 82 Hz), -127.2 (br. m) in an 11:1 ratio.

Synthesis of {(Dipp)(Mes)P}$_2$Ge·(*n*-hexane)$_{0.5}$ (1Ge): To a solution of (Dipp)(Mes)PH (0.81 g, 2.59 mmol) in THF (20 mL) was added a solution of *n*BuLi in hexanes (1.1 mL, 2.53 mmol). The resulting red solution was stirred for 1 h and then added, dropwise, to a solution of GeCl$_2$(1,4-dioxane) (0.30 g, 1.30 mmol) in THF (20 mL) and this mixture was stirred for 1 h. The solvent was removed *in vacuo* from the resulting dark red solution to give a sticky red solid. The product was extracted into *n*-hexane (20 mL) and filtered. The filtrate was reduced in volume to 5 mL and deposited large pale red crystals of **1Ge** suitable for X-ray crystallography on standing at room temperature overnight. A second crop of crystals was obtained by storing the mother liquor at -25 °C for 1 day. The supernatant solution was removed by filtration, the crystals were washed with cold (-10 °C) *n*-hexane (5 mL) and the residual solvent was removed under vacuum. Combined yield of crystals: 0.34 g, 35%. ^{1}H NMR: [d_8-toluene, 298 K]: δ 0.88 (t, J_{HH} = 7.0 Hz, 3H, *n*-hexane), 1.02 (d, J_{HH} = 6.8 Hz, 24H, CH*Me*$_2$), 1.21-1.28 (m, 4H, *n*-hexane), 2.06 (s, 6H, *p*-Me), 2.40 (s, 12H, *o*-Me), 3.44 (m, 4H, C*H*Me$_2$), 6.73 (s, 4H, ArH), 7.00 (d, J_{HH} = 7.5 Hz, 4H, ArH), 7.10 (m, 2H, ArH). ^{13}C{^{1}H} NMR: [d_8-toluene, 298 K]: δ 14.35 (*n*-hexane), 21.09 (*p*-Me), 23.11 (*n*-hexane), 24.88 (t, J_{PC} = 9.2 Hz, *o*-Me), 25.03 (CH*Me*$_2$), 32.05 (*n*-hexane), 33.80 (t, J_{PC} = 5.8 Hz, *C*HMe$_2$), 124.00, 128.51, 130.93 (Ar), 131.30 (t, J_{PC} = 12.0 Hz, Ar), 136.16 (t, J_{PC} = 6.4 Hz, Ar), 138.52 (Ar), 144.51 (t, J_{PC} = 4.6 Hz, Ar), 153.11 (t, J_{PC} = 4.2 Hz, Ar). ^{31}P{^{1}H} NMR: [d_8-toluene, 298 K]: δ -6.5 (br. s).

Synthesis of {(Dipp)(Mes)P}$_2$Sn (1Sn): To a solution of (Dipp)(Mes)PH (0.83 g, 2.66 mmol) in THF (15 mL) was added a solution of *n*BuLi in hexanes (2.3 M, 1.2 mL, 2.76

mmol). The resulting red solution was stirred for 1 h and added to a cold (-78 °C) solution of $SnCl_2$ (0.25 g, 1.33 mmol) in THF (15 mL), with the light excluded. The solution was allowed to warm to room temperature and the solvent was removed *in vacuo*. The product was extracted into methylcyclohexane (30 mL), the solution was filtered, and the filtrate was reduced in volume to 5 mL. Storage of this solution at -25 °C for 1 week gave large purple crystals of **1Sn** suitable for characterization by X-ray crystallography. The supernatant solution was removed by filtration and the purple crystals were washed with cold (0 °C) light petroleum (5 mL) and the residual solvent was removed under vacuum. Yield: 0.27 g, 27%. ^{1}H NMR [d_8-toluene, 298 K]: δ 0.97 (d, J_{HH} = 6.7 Hz, 24H, CH*Me*$_2$), 2.06 (s, 6H, *p*-Me), 2.43 (s, 12H, o-Me), 3.18 (sept, J_{HH} = 6.7 Hz, 4H, C*H*Me$_2$), 6.80 (s, 4H, ArH), 6.96 (d, J_{HH} = 7.8 Hz, 4H, ArH), 7.05 (d, J_{HH} = 7.8 Hz, 2H, ArH). ^{13}C{^{1}H} NMR [d_8-toluene, 298 K]: δ 21.14 (*p*-Me), 24.77 (*C*HMe$_2$), 25.49 (t, J_{PC} = 11.0 Hz, *o*-Me), 33.56 (t, J_{PC} = 5.5 Hz, *C*HMe$_2$), 123.50, 127.50 (Ar), 129.33 (m, Ar, partially obscured by solvent peak), 132.26 (Ar), 136.98 (m, Ar), 137.82 (Ar), 144.92 (t, J_{PC} = 4.5 Hz, Ar), 152.48 (t, J_{PC} = 4.4 Hz, Ar). ^{31}P{^{1}H} NMR [d_8-toluene, 298 K]: δ -53.5 ppm (J_{119SnP} = 855 Hz, J_{117SnP} = 816 Hz). ^{119}Sn{^{1}H} NMR [d_8-toluene, 298 K]: δ 476 (t, J_{SnP} = 855 Hz).

Synthesis of [(Dipp){(Me$_3$Si)$_2$CH}P]$_2$Sn (2Sn): To a cold (-78 °C) solution of (Dipp){(Me$_3$Si)$_2$CH}PH (0.63 g, 1.79 mmol) in THF (15 mL) was added a solution of *n*BuLi in hexanes (2.3 M, 0.8 mL, 1.84 mmol). The mixture was allowed to warm to room temperature and was stirred for 30 mins. The resulting red solution was added, dropwise, to a cold (-78 °C) solution of $SnCl_2$ (0.170 g, 1.79 mmol) in THF (15 mL) and this mixture was allowed to warm to room temperature. The solvent was removed *in vacuo* from the resulting orange solution to give a sticky orange solid. The product was extracted into toluene (10 mL) and the solution was filtered. The volume of the filtrate was reduced to 5 mL and this solution was stored at -25 °C for 1 week to give dark green crystals of **2Sn**. The supernatant

was decanted and the residual solvent was removed from the remaining solid under vacuum. Yield: 0.25 g, 34%. ^{1}H NMR [d_8-toluene, 298 K]: δ -0.01 (s, 36H, $SiMe_3$), 1.43 (br. s, 24H. $CHMe_2$), 1.96 (m, 2H, Si_2CH), 4.31 (s, 4H, $CHMe_2$), 7.05 (d, J_{HH} = 7.5 Hz, 4H, ArH), 7.12 (t, J_{HH} = 7.5 Hz, 2H, ArH). ^{13}C{^{1}H} NMR [d_8-toluene, 298 K]: δ 2.56 (m, $SiMe_3$), 10.72 (m, Si_2CH), 25.97, 27.26 (br. s, $CHMe_2$), 33.61 (t, J_{PC} = 9.5 Hz, $CHMe_2$), 125.58, 129.33 (Ar), 134.90 (m, Ar), 155.48 (Ar). ^{31}P{^{1}H} NMR [d_8-toluene, 298 K]: δ -30.1 (s, J_{SnP} = 1030 Hz).

Attempted synthesis of [{(Me$_3$Si)$_2$CH}$_2$P]$_2$Sn (3Sn): To a cold (-78 °C) solution of $SnCl_2$ (0.120 g, 0.63 mmol) in THF (10 mL) was added, dropwise, a solution of [{$(Me_3Si)_2CH$}$_2$P]Li(OEt_2) (0.500 g, 0.63 mmol) in THF (10 mL). The mixture was allowed to warm to room temperature to give a very dark red solution containing black solids. The solvent was removed *in vacuo*, the product was extracted into toluene (20 mL) and filtered. The solvent was removed *in vacuo* from the filtrate to give a dark red viscous oil, from which grew a small number of single crystals of **3Sn** after standing at room temperature for 16 h; one of these crystals was characterized by X-ray crystallography. ^{31}P{^{1}H} NMR spectrum (crude reaction mixture in THF, see main text): δ 43.2 (J_{PSn} = 1900 Hz).

X-ray crystallography: Crystal structure datasets for all compounds were collected on an Xcalibur, Atlas, Gemini ultra diffractometer using an Enhance Ultra X-ray Source ($\lambda_{CuK\alpha}$ = 1.54184 Å) for **1Ge**, **1Sn** and **3Sn** and a fine-focus sealed X-ray tube ($\lambda_{MoK\alpha}$ = 0.71073 Å) for **2Li**, and **2Sn**. Using an Oxford Cryosystems CryostreamPlus open-flow N_2 cooling device, data for all structures were collected at 150 K. Cell refinement, data collection and data reduction were undertaken using CrysAlisPro.[24] For **1Ge**, **1Sn** and **2Sn** an analytical numeric absorption correction was applied using a multifaceted crystal model based on expressions derived by R. C. Clark and J. S. Reid.[25] For **2Li** and **3Sn** intensities were corrected for absorption empirically using spherical harmonics. The structures were solved using XT[26] and refined by XL[27] through the Olex2 interface.[28] Hydrogen atoms were

positioned with idealized geometry and their displacement parameters were constrained using a riding model.

DFT calculations: Geometry optimizations were performed with the Gaussian09 suite of programs (revision D.01).[29] The pure B97D functional,[30] which includes a correction for dispersion effects, was employed throughout; the 6-311G(2d,p) all-electron basis set[31] was used on all atoms except Sn, for which the relativistic lanl2dz basis set[32] was used [default parameters were used throughout]. The identity of minima was confirmed by the absence of imaginary vibrational frequencies in each case. Automatic density fitting was employed for all geometry optimizations and frequency calculations. Natural Bond Orbital analyses were performed using the NBO 3.1 module of Gaussian09.[33]

Acknowledgement: This work was part-funded by the UK Engineering and Physical Sciences Research Council (EPSRC; EP/L5048281).

Supporting Information: Crystallographic details for **1Ge**, **1Sn**, **2Li**, **2Sn** and **3Sn** in tabular format. ^{1}H, ^{13}C{^{1}H}, and ^{31}P{^{1}H} NMR spectra of all compounds and ^{7}Li and ^{119}Sn{^{1}H} NMR spectra where applicable. Structures, final atomic coordinates and energies for all calculated geometries and selected tabulated data. This material is available free of charge via the Internet at http://pubs.acs.org.

Accession Codes: CCDC 1958750-1958754 contain the supplementary crystallographic data for this paper. These data can be obtained free of charge via www.ccdc.cam.ac.uk/data_request/cif, or by emailing data_request@ccdc.cam.ac.uk, or by contacting The Cambridge Crystallographic Data Centre, 12 Union Road, Cambridge CB2 1EZ, UK; fax: +44 1223 336033.

AUTHOR INFORMATION Corresponding Author *E-mail: keith.izod@ncl.ac.uk.

ORCID Keith Izod: 0000-0003-3882-9343, Peter Evans: 0000-0002-5916-8786.

Notes The authors declare no competing financial interest.

References:

1. For reviews see: (a) Vignolle, J.; Cattoën, X.; Borrissou, D. Stable Noncyclic Singlet Carbenes. *Chem. Rev.* **2009**, *109*, 3333-3384. (b) Martin, D.; Melami, M.; Soleilhavoup, M.; Bertrand, G. A Brief Survey of Our Contribution to Stable Carbene Chemistry. *Organometallics* **2011**, *30*, 5304-5313. (c) Melaimi, M.; Soleilhavoup, M.; Bertrand, G. Stable Cyclic Carbenes and Related Species Beyond Diaminocarbenes. *Angew. Chem. Int. Ed.* **2010**, *49*, 8810-8849.
2. (a) Martin, D.; Baceiredo, A.; Gornitzka, H.; Schoeller, W. W.; Bertrand, G. A Stable P-Heterocyclic Carbene. *Angew. Chem., Int. Ed.* **2005**, *44*, 1700-1703. (b) Masuda, J. D.; Martin, D.; Lyon-Saunier, C.; Baceiredo, A.; Gornitzka, H.; Donnadieu, B.; Bertrand, G. Stable P-Heterocyclic Carbenes: Scope and Limitations. *Chem.-Asian J.* **2007**, *2*, 178-187.
3. For recent reviews see: (a) Izod, K. Heavier group 14 complexes with anionic P-donor ligands. *Coord. Chem. Rev.* **2012**, *256*, 2972-2993. (b) Rosenberg, L. Metal complexes of planar PR_2 ligands: Examining the carbene analogy. *Coord. Chem. Rev.* **2012**, *256*, 606-626.
4. (a) duMont, W.-W.; Kroth, K. J. Dimeric Bis(di-*tert*-butylphosphino)stannanediyl: A Cyclic Phosphorus-Tin Ylide. *Angew. Chem. Int. Ed. Engl.* **1977**, *16*, 792-793. (b) duMont, W.-W.; Grenz, M. Dimere Phospha- und Thiastannylene: Ylidartige Diphospha- und Dithiadistannetan. *Chem. Ber.* **1985**, *118*, 1045-1049. (c) Arif, A. M.; Cowley, A. H.; Jones, R. A.; Power, J. M. Bis(t-butyl)phosphido Complexes of Tin(II) and Lead(II); Analogues of Lithium-complexed Carbanions. *J. Chem. Soc. Chem. Commun.* **1986**, 1446-1447. (d) Cowley, A. H.; Giolando, D. M.; Jones, R. A.; Nunn, C. M.; Power, J. M. Synthesis and Structure of $[Pb(\mu\text{-}P\text{-}t\text{-}Bu_2)P\text{-}t\text{-}Bu_2]_2$. *Polyhedron* **1988**, *7*, 1909-1910. (e) Goel, S. C.; Chiang, M. Y.; Rauscher, D. J.; Buhro, W. E.

Comparing the Properties of Homologous Phosphido and Amido Complexes: Synthesis and Characterization of the Disilylphosphido Complexes $\{M[P(SiMe_3)_2]_2\}_2$ Where M = Zn, Cd, Hg, Sn, Pb, and Mn. *J. Am. Chem. Soc.* **1993**, *115*, 160-169. (f) Westerhausen, M.; Enzelberger, M. M.; Schwarz, W. Reaktivität von Magnesium und Calcium-bis[bis(trimethylsilyl)phosphanid] gegenüber Bis[bis(trimethylsilyl)aminolstannylen in Toluollösung. *J. Organomet. Chem.* **1995**, *491*, 83-90. (g) Druckenbrodt, C.; duMont, W.-W.; Ruthe, F.; Jones, P.G. Dimere Dialkylphosphanylgermylene: Ylidische Diphosphadigermetane. *Z. Anorg, Allg. Chem.* **1998,** *624*, 590-594. (h) Izod, K.; Stewart, J.; Clark, E. R.; Clegg, W.; Harrington, R. W. Germanium(II) and Tin(II) Complexes of a Sterically Demanding Phosphanide Ligand. *Inorg. Chem.* **2010**, *49*, 4698-4707. (i) Johnson, B. P.; Almstatter, S.; Dielmann, F.; Bodensteiner, M.; Scheer, M. Synthesis and Reactivity of Low-Valent Group 14 Element Compounds. *Z. Anorg. Allg. Chem.* **2010**, *636*, 1275-1285.

5. Driess, M.; Janoschek, R.; Pritzkow, H.; Rell, S.; Winkler, U. Diphosphanyl- and Diarsanyl-Substituted Carbene Homologues: Germanediyls, Stannanediyls, and Plumbanediyls with Remarkable Electronic Structures. *Angew. Chem. Int. Ed.* **1995**, *34*, 1614-1616.

6. (a) Matchett, M. A.; Chiang, M. Y.; Buhro, W. E. Disilylphosphido Complexes $M[P(SiPh_3)_2]_2$, Where M = Zn, Cd, Hg, and Sn: Effective Steric Equivalency of $P(SiPh_3)_2$ and $N(SiMe_3)_2$ Ligands. *Inorg. Chem.* **1994**, *33*, 1109-1114. (b) Rivard, E.; Sutton, A. D.; Fettinger, J. C.; Power, P.P. Synthesis of the sterically congested diarylphosphines $Ar^{Trip2}P(Ph)H$ ($Ar^{Trip2} = C_6H_3$-2,6(C_6H_2-2,4,6-Pr^i_3)) and $Ar^{Mes2}P(Ph)H$ ($Ar^{Mes2} = C_6H_3$-2,6(C_6H_2-2,4,6-Me_3)) and the monomeric Sn(II)-diphosphide $[Ar^{Mes2}P(Ph)]_2Sn$ *Inorg. Chim. Acta* **2007**, *360*, 1278-1286.

7. (a) Izod, K.; McFarlane, W.; Allen, B.; Clegg, W.; Harrington, R. W. An Intramolecularly Base-Stabilized Diphosphagermylene and Two Unusual Germanium(II) Ate Complexes: A Structural, NMR, and DFT Study. *Organometallics* **2005**, *24*, 2157-2167. (b) Izod, K.; Stewart, J.; Clark, E. R.; McFarlane, W.; Allen, B.; Clegg, W.; Harrington, R. W. Dynamic Behavior of Intramolecularly Base-Stabilized Phosphatetrylenes. Insights into the Inversion Processes of Trigonal Pyramidal Germanium(II) and Tin(II) Centers. *Organometallics* **2009**, *28*, 3327-3337. (c) Izod, K.; Stewart, J.; Clegg, W.; Harrington, R. W. Synthesis, Structures, and Dynamic Behavior of Intramolecularly Base-Stabilized Diphosphatetrylenes Containing a Five-Membered Chelate Ring. *Organometallics* **2010**, *29*, 108-116. (d) Izod, K.; Clark, E. R.; Clegg, W.; Harrington, R. W. Hypervalent Sulfur-Functionalized Diphosphagermylene and Diphosphastannylene Compounds. *Organometallics* **2012**, *31*, 246-255.

8. Schwarz, E.; Mueller, S.; Weinberger, G.; Torvisco, A.; Flock, M. Synthesis and theoretical investigation of diphosphastannylenes. *Organometallics* **2018**, *37*, 2950-2960.

9. Řezníček, T.; Dostál, L.; Růžička, A.; Jambor, R. Diphosphastannylenes: Precursors for Phosphorus–Phosphorus Coupling? *Eur. J. Inorg. Chem.* **2012**, 2983-2987.

10. Greenwood, N. N.; Earnshaw, A. *Chemistry of the elements* 2nd Ed. Butterworth-Heinmann: Oxford, 1997, p. 493.

11. Izod, K.; Rayner, D. G.; El-Hamruni, S. M.; Harrington, R. W.; Baisch, U. Stabilization of a diphosphagermylene through pπ-pπ interactions with a trigonal planar phosphorus center. *Angew. Chem. Int. Ed.* **2014**, *53*, 3636-3640.

12. Izod, K.; Evans, P.; Waddell, P. G.; Probert, M. R. Remote substituent effects on the structures and stabilities of P=E π-stabilized diphosphatetrylenes $(R_2P)_2E$, E = Ge, Sn. *Inorg. Chem.* **2016**, *55*, 10510-10522.

13. Izod, K.; Evans, P.; Waddell, P. G. Desolvation and aggregation of sterically demanding alkali metal diarylphosphides. *Dalton Trans.* **2017**, *46*. 13824-13834.

14. Mantina, M.; Chamberlain, A. C.; Valero, R.; Cramer, C. J.; Truhlar, D. G. Consistent van der Waals radii for the whole main group. *J. Phys. Chem. A* **2009**, *113*, 5806-5812.

15. Izod, K.; Evans, P.; Waddell, P. G. A diarsagermylene and a diarsastannylene stabilized by arene···Ge/Sn interactions. *Chem. Commun.* **2018**, *54*, 2526-2529.

16. We exclude dimerization of **1Ge** as an explanation for the observed dynamic equilibria on the basis of the following: (i) a space-filling model of **1Ge** shows the germanium center to be shrouded by the ligands and so it is unlikely to be accessible for dimer formation (especially when this would involve either further coordination of a very bulky ligand to give a dimer with a Ge_2P_2 core or else the direct approach of two very hindered germanium centers to give a digermene with a Ge=Ge bond); (ii) dimerization via a Ge_2P_2 core should give rise to an A_2B_2 splitting pattern in the low temperature $^{31}P\{^1H\}$ NMR spectrum of **1Ge**, whereas only a singlet is observed (in addition to signals due to the planar/pyramidal form of this compound); (iii) in dimeric diphosphagermylenes containing an E_2P_2 core such as $(t\text{Bu}_2\text{P})\text{Pb}(\mu\text{-}t\text{Bu}_2\text{P})_2\text{Pb}(\text{P}t\text{Bu}_2)$ bridging-terminal ligand exchange is not observed (reference 4d).

17. For selected articles on P/As inversion see: (a) Beachler, R. D.; Mislow, K. Barrier to Pyramidal Inversion in Silylphosphines. *J. Am. Chem. Soc.* **1970**, *92*, 4758-4759. (b) Beachler, R. D.; Mislow, K. Effect of Ligand Electronegativity on the Inversion Barrier of Phosphines. *J. Am. Chem. Soc.* **1971**, *93*, 773-774. (c) Beachler, R. D.; Casey, J. P.; Cook, R. J.; Senkler, G. H. Jr.; Mislow, K. Effect of Ligand Electronegativity on the

Inversion Barriers of Arsines. *J. Am. Chem. Soc.* **1972**, *94*, 2859-2861. (d) Beachler, R. D.; Andose, J. D.; Stackhouse, J.; Mislow, K. Linear Free Energy Correlations of Barriers to Pyramidal Inversion. *J. Am. Chem. Soc.* **1972**, *94*, 8060-8065. (e) Izod, K.; Clark, E. R.; Stewart, J. Edge- versus Vertex-Inversion at Trigonal Pyramidal Ge(II) Centers— A New Aromatic Anchimerically Assisted Edge-Inversion Mechanism. *Inorg. Chem.* **2011**, *50*, 3651-3661.

18. (a) Gómez-Suárez, A.; Nelson D. J.; Nolan, S. P. Quantifying and understanding the steric properties of N-heterocyclic carbenes. *Chem. Commun.* **2017**, *53*, 2650-2660. (b) Poater, A.; Cosenza, B.; Correa, A.; Giudice, S.; Ragone, F.; Scarano, V.; Cavallo, L. SambVca: A web application for the calculation of the buried volume of N-heterocyclic carbene ligands. *Eur. J. Inorg. Chem.* **2009**, 1759-1766.

19. Gynane, M. J. S.; Hudson, A.; Lappert, M. F.; Power, P. P.; Goldwhite, H. Bulky alkyls, amides, and aryloxides of main Group 5 elements. Part 1. Persistent phosphinyl and arsinyl radicals ·MRR′ and their chloroprecursors MRR′Cl and related compounds. *J. Chem. Soc. Dalton Trans.* **1980**, 2428-2433.

20. Bartlett, R. A.; Dias, H. V. R.; Power, P. P. Isolation and X-ray crystal structures of the organolithium etherate complexes, $[Li(Et_2O)_2(CPh_3)]$ and $[\{Li(Et_2O)(2,4,6\text{-}(CHMe_2)_3C_6H_2)\}_2]$. *J. Organomet. Chem.* **1988**, *341*, 1-9.

21. For a review see: Izod, K. Group 1 complexes of P- and As-donor ligands. *Avd. Inorg. Chem.* **2012**, *50*, 33-108.

22. Hitchcock, P. B.; Lappert, M. F.; Power, P. P.; Smith, S. J. Synthesis, structure and reactivity of a μ-bis(dialkylphosphido)-dilithim $[Li(\mu\text{-}PR_2)]_2$ [R = $CH(SiMe_3)_2$]. *J. Chem. Soc., Chem. Commun.* **1984**, 1669-1670.

23. Pestana, D.C.; Power, P. P. Synthesis and Structure of Diarylboryl-Substituted Hydrazines and Diphosphanes: Role of σ-Orbital Hybridization and π-Orbital Overlap in N-N and P-P Multiple-Bond Lengths. *Inorg. Chem.* **1991**, *30*, 528-535.

24. CrysAlisPro, Agilent Technologies, Version 1.171.36.

25. Clark R. C.; Reid, J. S. The analytical calculation of absorption in multifaceted crystals. *Acta Cryst.* **1995**, *A51*, 887-897.

26. Sheldrick, G. M. SHELXT – Integrated space-group and crystal-structure determination. *Acta Cryst.* **2015**, *A71*, 3-8.

27. Sheldrick, G. M. A short history of SHELX. *Acta Cryst.* **2008**, *A64*, 112-122.

28. Dolomanov, O. V.; Bourhis, L. J.; Gildea, R. J.; Howard J. A. K.; Puschmann, H. OLEX2: a complete structure solution, refinement and analysis program. *J. Appl. Cryst.*, **2009**, *42*, 339-341.

29. Gaussian 09, Revision D.01, Frisch, M. J.; Trucks, G. W.; Schlegel, H. B.; Scuseria, G. E.; Robb, M. A.; Cheeseman, J. R.; Scalmani, G.; Barone, V.; Mennucci, B.; Petersson, G. A.; Nakatsuji, H.; Caricato, M.; Li, X.; Hratchian, H. P.; Izmaylov, A. F.; Bloino, J.; Zheng, G.; Sonnenberg, J. L.; Hada, M.; Ehara, M.; Toyota, K.; Fukuda, R.; Hasegawa, J.; Ishida, M.; Nakajima, T.; Honda, Y.; Kitao, O.; Nakai, H.; Vreven, T.; Montgomery, J. A., Jr.; Peralta, J. E.; Ogliaro, F.; Bearpark, M.; Heyd, J. J.; Brothers, E.; Kudin, K. N.; Staroverov, V. N.; Kobayashi, R.; Normand, J.; Raghavachari, K.; Rendell, A.; Burant, J. C.; Iyengar, S. S.; Tomasi, J.; Cossi, M.; Rega, N.; Millam, N. J.; Klene, M.; Knox, J. E.; Cross, J. B.; Bakken, V.; Adamo, C.; Jaramillo, J.; Gomperts, R.; Stratmann, R. E.; Yazyev, O.; Austin, A. J.; Cammi, R.; Pomelli, C.; Ochterski, J. W.; Martin, R. L.; Morokuma, K.; Zakrzewski, V. G.; Voth, G. A.; Salvador, P.;

Dannenberg, J. J.; Dapprich, S.; Daniels, A. D.; Farkas, Ö.; Foresman, J. B.; Ortiz, J. V.; Cioslowski, J.; Fox, D. J. Gaussian, Inc., Wallingford CT, **2009**.

30. Grimme, S. Semiempirical GGA-type density functional constructed with a long-range dispersion correction. *J. Comput. Chem.* **2006**, *27*, 1787-1799.

31. (a) McLean, A. D.; Chandler, G. S. Contracted Gaussian basis sets for molecular calculations. I. Second row atoms, *Z*=11–18. *J. Chem. Phys.* **1980**, *72* 5639-5648. (b) Raghavachari, K.; Binkley, J. S.; Seeger, R.; Pople, J. A. Self-consistent molecular orbital methods. XX. A basis set for correlated wave functions. *J. Chem. Phys.*, **1980**, *72*, 650-654. (c) Binning Jr., R. C.; Curtiss, L. A. Compact contracted basis sets for third-row atoms: Ga–Kr. *J. Comput. Chem.* **1990**, *11*, 1206-1216; (d) Curtiss, L. A.; McGrath, M. P.; Blaudeau, J.-P.; Davis, N. E.; Binning Jr., R. C.; Radom, L. Extension of Gaussian-2 theory to molecules containing third-row atoms Ga–Kr. *J. Chem. Phys.* **1995**, *103*, 6104-6113.

32. (a) Hay, P. J.; Wadt, W. R. *Ab initio* effective core potentials for molecular calculations. Potentials for the transition metal atoms Sc to Hg. *J. Chem. Phys.* **1985**, *82*, 270-283. (b) Wadt, W. R.; Hay, P. J. *Ab initio* effective core potentials for molecular calculations. Potentials for main group elements Na to Bi. *J. Chem. Phys.* **1985**, *82*, 284-298. (c) Hay, P. J.; Wadt, W. R. Ab initio effective core potentials for molecular calculations. Potentials for K to Au including the outermost core orbitals. *J. Chem. Phys.* **1985**, *82*, 299-310.

33. NBO Version 3.1, Glendening, E. D.; Reed, A. E.; Carpenter, J. E.; Weinhold, F.

For Table of Contents use only:

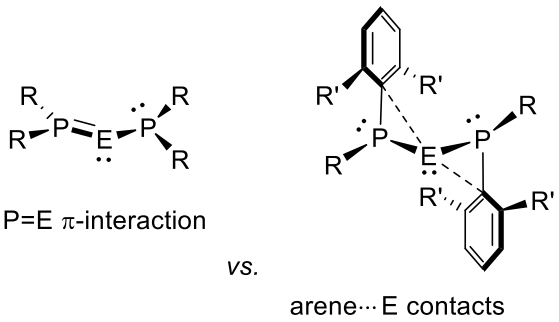

Structural, NMR and DFT studies reveal competition between P=E π-interactions and arene···E contacts for the stabilization of diphosphatetrylenes. These studies show that the tendency for either interaction is at least partially determined by the steric properties of the ligands.